DESIGN OF STAINLESS STEEL WELDING CONSUMABLES FOR CRYOGENIC SERVICE

by

S. CHAKRAVARTY, T.P.S. GILL, A.K. JOSEPH*, PENNATHUR* AND N.T. SEBASTIAN*

Materials Development Division
Indira Gandhi Centre for Atomic Research, Kalpakkam 603 102
*Kemtrode Pvt. Ltd., Bangalore 560 001

Abstract

Austenitic stainless steels are commonly used as structural materials for cryogenic temperature application. The components fabricated using welding require that the welds should have desirable properties at cryogenic temperatures. This necessitates the selection of right type of electrodes to provide a weld metal with beneficial properties such as tensile strength and impact properties. The various factors which characterize the weld metal such as solidification mechanism, optimum control of delta ferrite, resistance to hot cracking, minimum inclusion content, type of coating, heat input and the addition of rare earths are discussed with a view to elucidating the effect of these in improving the weld metal performance.

INTRODUCTION

Among the family of stainless steels, austenitic stainless steels (ASS) are the only Fe-Cr-Ni alloys suitable for cryogenic applications. These steels contain 16-25% Cr, 7-20% Ni and often have reduced carbon content. Further, they are frequently alloyed with Mo, Ti and Nb to impart some special properties and stabilization against intergranular corrosion.

Stainless steel welds intended for low temperature service must exhibit certain desirable characteristics in addition to satisfactory engineering properties such as, yield and tensile strengths. Low carbon, controlled ferrite and minimum inclusion content are the significant parameters, which need to be controlled to achieve the desirable cryogenic properties.

In this paper, an attempt is made to explain the significance of the effect of individual alloying elements, heat input during welding, coating characteristics of the electrodes, on the weld metal behaviour in order to achieve the above mentioned properties. Furthermore, beneficial effects due to the addition of some strong deoxidisers like rare earths (RE) in welds are also discussed. REs take precedence to form compounds that prevent the presence of low melting inclusions in the weld metal. This contributes to improved resistance to solidification cracking and an appreciable increase in mechanical properties even at cryogenic temperatures.

SOLIDIFICATION OF AUSTENITIC STAINLESS STEELS

Solidification Mechanism

Understanding of the Fe-Cr-Ni diagram is required to study the solidification mechanism of stainless steels. A vertical section of Fe-Cr-Ni ternary equilibrium system at 70 wt% Fe (**Fig. 1**) shows possible sequences of phase separation during solidification under equilibrium conditions for various alloy compositions. However, the solidification behaviour and sequences of phase separation in austenitic stainless steel weld-metal depart considerably from this phase diagram due to the presence of other alloying elements as well as due to the rapid cooling of the weld-metal.

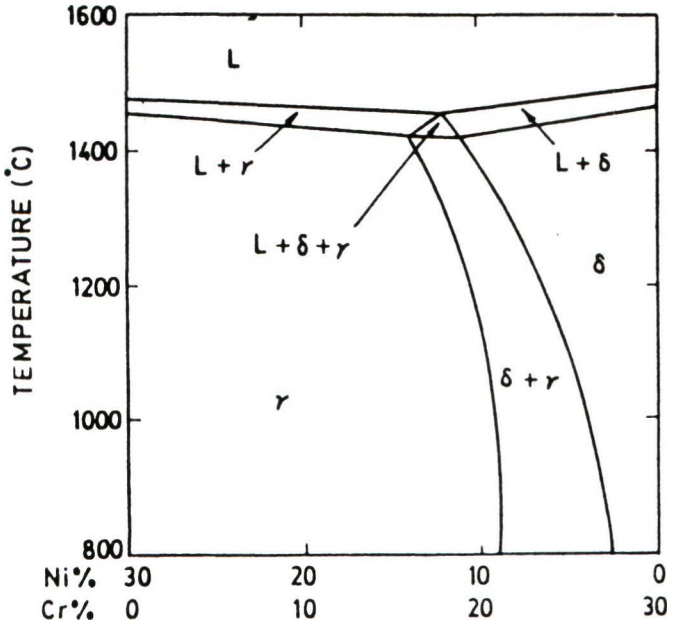

Fig. 1 : Vertical section of the Fe-Cr-Ni phase diagram at 70%Fe.

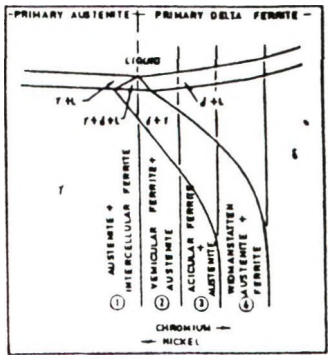

Fig. 2 : Vertical section of the Fe-Cr-Ni phase diagram illustration the effect of composition of austenite-ferrite morphology.

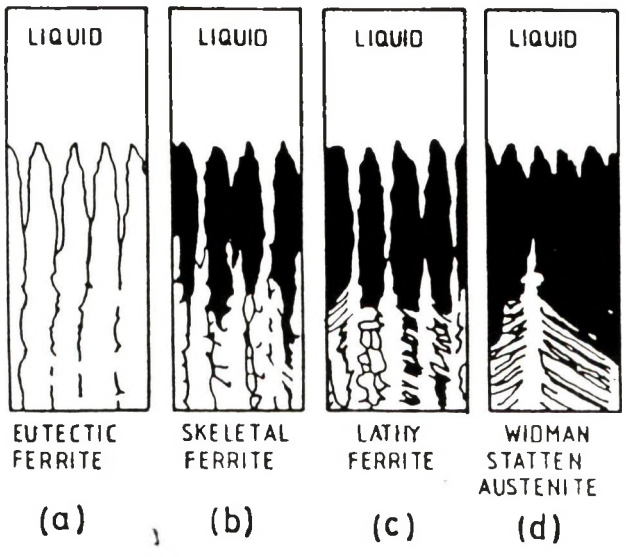

Fig. 3 : The sequence of formation of structure varying (Cr/Ni) equivalent, a) Distorted eutectic, b) Vermicular, c) Acicular and d) Widmanstatten

The effect of composition on austenite-ferrite morphology in ASS weld metals is schematically represented as different zones in **Fig. 2** that predicts the behaviour of a wide range of alloy systems upon cooling in the solidification range.

Alloys in Zone 1 (**Fig. 2**) solidify as primary austenite (**Fig. 3a**) and may form a limited amount of ferrite as a divorced eutectic along the intercellular boundaries (**Fig. 4a**). However, alloys in Zone 2 (**Fig. 2**) solidify as primary delta ferrite dendrites (**Fig. 3b**) whose cores are highly enriched in chromium and depleted in nickel. On cooling through the two phase (A+F) region, the ferrite of normal composition formed during steady state solidification may transform to austenite by a composition invariant massive transformation. A portion of the ferrite at the dendritic cores, sufficiently

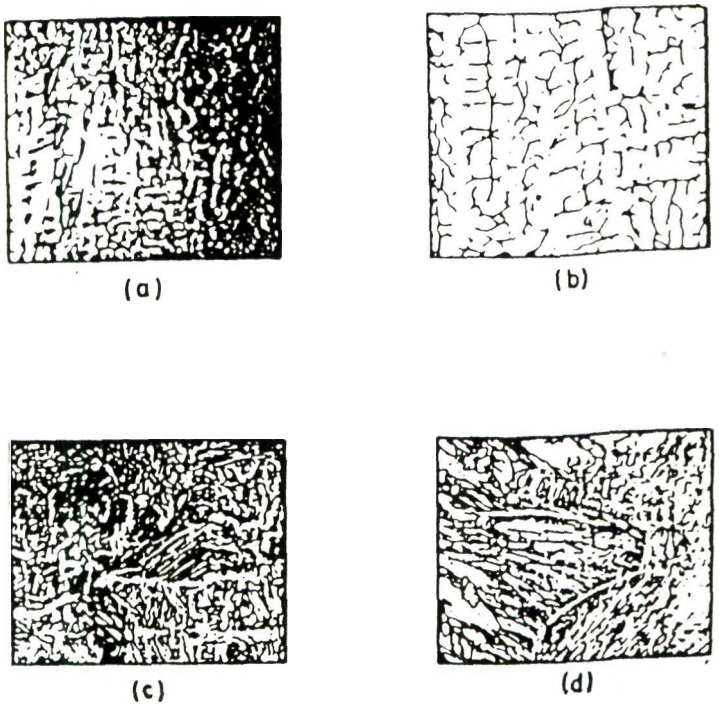

Fig. 4 : The microstructure of ASS weld metal as a function of increasing Cr_{eq}/Ni_{eq} ratio, at X 500 a) Distorted eutectic, b) Vermicular, c) Acicular and d) Widsmantatten [36]

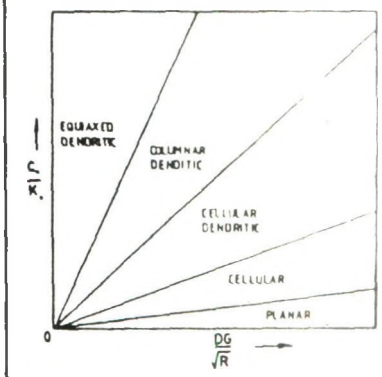

Fig. 5 : Schematic representation of solidification patterns as a function of thermal and constitutional variables. Where C_o/K_o is the segregation parameter (KO - partition co-efficient), D-diffusion co-efficient, G-thermal gradient and R-rate of growth.

enriched in Chromium and depleted in Nickel, still remains stable at room temperature and is characterized by a vermicular morphology (**Fig. 4b**). As the Cr/Ni ratio increases within this region, the ferrite network becomes more continuous. For alloys in Zone-3 (**Fig. 2**), the primary delta ferrite is stable over relatively large temperature range and diffusion occurs during cooling from solidus to the ferrite solvus through a smooth concentration gradient.

However, the cooling rate through the two phase region still suppresses the diffusion controlled transformation of the ferrite (**Fig. 3c**) and an acicular morphology exists in the microstructures at room temperature (**Fig. 4c**). The ferrite and austenite co-exist in a near equilibrium mixture at room temperature in the Zone-4 (**Fig. 2**). Since the composition of the austenite formed differs from the nominal composition, a massive transformation is not possible in these alloys. consequently, a diffusion controlled transformation of ferrite to austenite must occur through the two phase region (**Fig. 3d**) and the as-welded microstructure consists of ferrite and Widmanstatten austenite (**Fig. 4d**).

The solidification process during welding proceeds by epitaxial growth from the base metal grains. The morphology of growth from liquid phase to solid phase is dependent on: (i) heat flow conditions such as thermal gradient and cooling rate; and (ii) the chemical characteristics of the metal viz. composition (C), partition coefficient (K), and diffusivities (D) of the constituent solute species. The constitutional supercooling arises from the solidification front and leads to instability at the planar solid-liquid

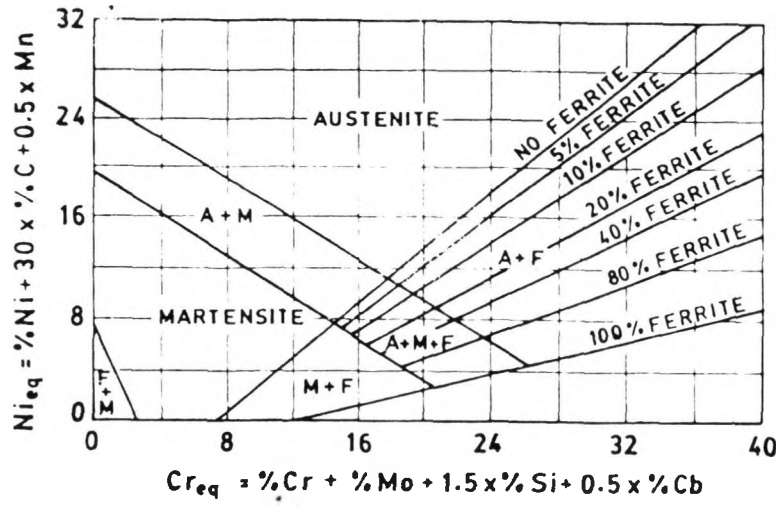

Fig. 6 : The Schaeffler constitution diagram for stainless steel weld metal

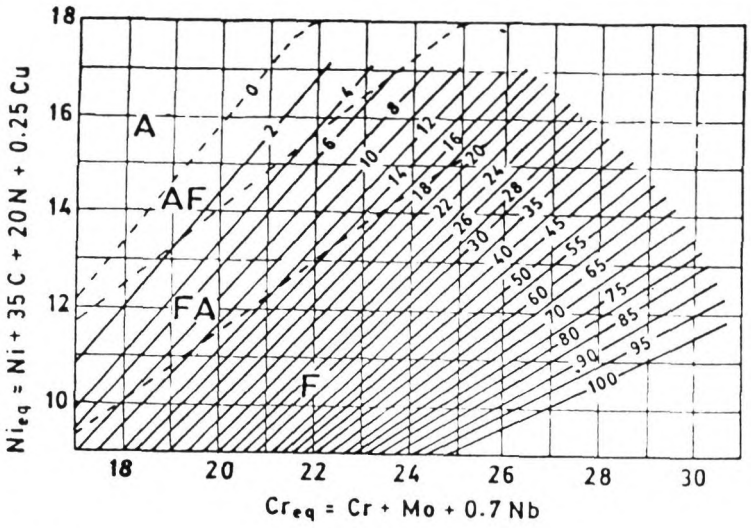

Fig. 7 : RWC-1992 constitution diagram for stainless steel weld metal

interface, and results in a variety of growth morphologies. This is schematically shown in **Fig. 5** as a function of kinetic and compositional variables.

Measurement of Delta-Ferrite

Delta-ferrite originates during solidification of most types of austenitic stainless steels. The fast cooling rate characteristics of welding leads to non-equilibrium structure. Therefore, the quantity and chemical composition of ferrite obtained in weld zone also differ from the equilibrium structure. The features of ferrite also change in multi-run welds or in heat-treated welds depending on the thermal history of the weld. The various methods for the estimation of ferrite are briefly described below.

Constitutional diagrams : *The alloying elements present in the ASS can be classed either as austenite formers (N, C, Cu, Ni, Co, Mn) or as ferrite formers (Mo, W, Nb, Cr, Ti, V, Si, Al). The contribution of austenite stabilisers is represented by nickel equivalent and the ferrite stabilisers by chromium equivalent. The values are plotted on the constitutional diagram to find out the ferrite number.* Schaeffler diagram (**Fig. 6**) *was the first of its kind to determine the ferrite content of the stainless steel weld metals. DeLong diagram includes the effect of nitrogen also and provides more accurate results for high alloyed grades. The Welding Research Council proposed WRC-1992 diagram (***Fig. 7***) where the effect of copper is also considered (1). In this diagram the nickel and chromium equivalent formulae are simplified considering the interactive effects of elements.*

Quantitative metallography : *The technique is based on the assumption that the volumetric proportion of 3-dimensional aggregate is equal to proportion viewed on a random 2-dimensional plane (2). The assumption is often not valid and conversion factor is established for the calculation of volume proportion from area. Also, this technique can not effectively differentiate between non-*

transformed and partly transformed ferrite (3,4). The products of transformed ferrite (sigma, chi or carbides) are usually counted as ferrite and the true ferrite content frequently is lower than the ferrite determined by quantitative metallography.

X-ray diffraction : This method is normally used for exact quantitative determination of the content of certain phases in two-phase or polyphase alloys. But it is not found suitable for ferrite determination of ASS weld metal (5,6,7). The limitations of analysis in welds are due to inhomogeneity, preferred orientation, internal stresses and simultaneous presence of the other secondary phases. Moreover, the measurements are made in a narrow area and the information derived is either from surface or sub-surface.

Saturation magnetisation : The method is based on the principle that the intensity of saturation of a two-phase material containing one ferromagnetic and the other non-magnetic phase is proportional to the content of the former phase and is independent of shape, size and orientation of the ferromagnetic particles (8,9,5,2).

This method is the best available method for accurate and absolute measurement of ferrite content. But, limitations of this method for everyday routine measurements are that the equipment is expensive and requires frequent calibration.

Permeability : The overall permeability of a two phase alloy containing one ferromagnetic and the other non-ferromagnetic phase depends, at a given strength of magnetic field, upon the individual permeability, content and demagnetization factor of the ferromagnetic phase (9). The relation is expressed as :

$\mu = 1 + \text{constant} * F/N$

where,

μ = Overall permeability of a two-phase sample

F = Content of ferromagnetic phase in the two phase sample

N = Demagnetisation factor depends upon the shape, especially upon the ratio of diameter and length

Attractive force : An attractive force acts between a ferromagnetic material and a permanent magnet. This phenomenon is utilised for the measurement of ferrite content in austenitic stainless steels. The overall permeability of the largely austenitic weld metal serves as an indicator of ferrite content. It depends more sensitively on quantity, shape, size and orientation of the ferromagnetic phase than its chemical composition (8,10). The relation between attractive force and the overall permeability of mostly austenitic weld metal is given by the equation

$F = C(\mu - 1)$

where,

F = Attractive force

C = A constant depending upon the strength and the size of the permanent magnet, the distance and the size of the 2-phase specimen

μ = Overall permeability of the 2-phase specimen

All methods based on this principle yield an arbitrary ferrite content. The relationship considering alloyed ferrite is not established and calibration of magnetic instruments is necessary to yield reasonably true ferrite content.

Mossbauer effect : It is a technique measuring resonant nuclear gamma ray fluorescence in solids utilising a Mossbauer spectrometer [6]. When a sample contains two or more phases and each of them gives a well resolved Mossbauer spectrum, the relative areas of the spectral patterns provide an indication of the amount of each phase present. If one of the phases is ferrite and the other austenite in Cr-Ni weld metal, the values of ferrite content obtained depend on chemical composition of ferrite rather than shape, size and orientation. It is basically a surface technique probing the sample upto a few hundredth of a millimeter. The precision is reported to be poorer than saturation magnetisation. The method is not extensively used for ferrite determination and needs further development.

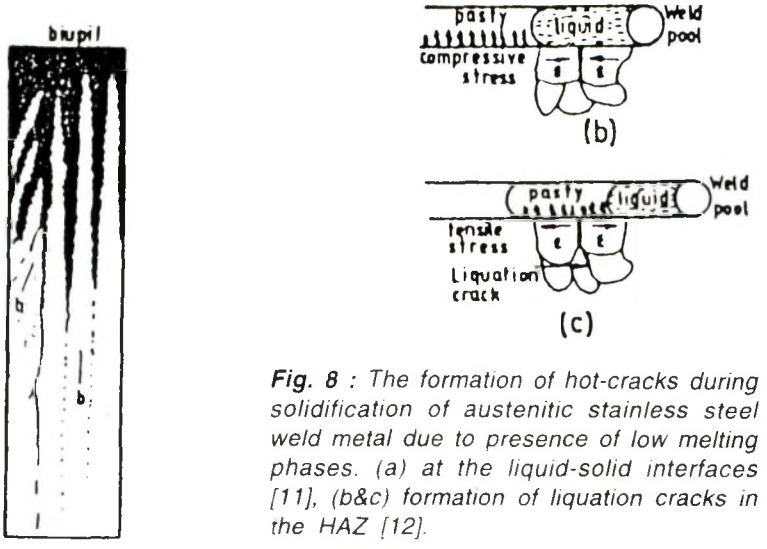

Fig. 8 : The formation of hot-cracks during solidification of austenitic stainless steel weld metal due to presence of low melting phases. (a) at the liquid-solid interfaces [11], (b&c) formation of liquation cracks in the HAZ [12].

ε = deformation by shrinkage

d = direction of crystallisation

Table - 1

The constitution and melting points of possible low melting phases

Constituent	Structure	Melting Point (°C)
Sulphur	Eutectic Fe-FeS	988
	Eutectic Ni-NiS	630
Phosphorus	Eutectic Fe-Fe_3P	1048
	Eutectic Ni-Ni_3P	875
Boron	Eutectic Fe-Fe_2B	1177
	Eutectic Ni-Ni_2B	1140
	Eutectic $(Fe, Cr)_2$ B-Austenite	1180
Niobium	Eutectic Fe-Fe_2Nb	1370
	Eutectic NbC-Austenite	1315
	Nb-Ni rich phase	1160
Titanium	Eutectic Fe-Fe_2Ti	1290
	Eutectic TiC-Austenite	1320
Silicon	Eutectic Fe-Fe Si	1212
	Eutectic NiSi-Ni Si	964
	Eutectic NiSi-NiSi	996

Hot Cracking in Austenitic Stainless Steel Weldments

The hot cracking phenomenon during the welding of ASS can be divided into two types differing in respect of their location in a weldment :

1. Solidification cracks in weld metal
2. Liquation cracks in heat affected zone
   a. of base metal and
   b. of weld metal of previously deposited passes

Solidification cracking occurs either at the junction of differently oriented dendrites or in the interdendritic regions. The cause of cracking is found in the metallurgically dependent formation of low melting phases which form a liquid film at the grain boundaries of the primary solidified crystals. **Fig. 8a** shows a schematic represe- ntation according to Arata et al. [11] of the formation of hot cracks in fully austenitic weld metal. The liquid phases settle between the dendritic branches where the liquid-solid interfaces of the crystals meet.

According to Apblett and Pellini [12], liquation crack in the HAZ of the base metal are formed by the grain boundary segregations which lead to the formation of low melting phases at the grain boundaries. During deposition of the subsequent weld beads, the segregants become locally liquefied again and the fused low melting phases will produce material segregation during the shrinkage process. This is schematically shown in **Fig. 8b** and **Fig. 8c**. During welding, the HAZ is subjected to compressive stresses but tensile stresses are developed at the latter point, normally after solidification of the weld metal.

If the transition temperature from compressive to tensile stresses is lowered, the remelted liquid phase gets solidified and no separation of the crystal structure

occurs. But if welds cool rapidly, as happens with thicker materials, the temperature at the time of changeover from compressive to tensile will be high and possibility of liquid phase remaining at the grain boundaries will be higher.

Effect of alloying elements and impurities on cracking : A general survey of the influence of alloying elements on hot cracking sensitivity of ASS is given by Hull [13], Borland and Younger [14] and by Thomas [15]. The main elements that increase the hot cracking susceptibility are sulphur, phosphorus, boron, silicon, niobium and titanium. The low melting phases formed by these elements at elevated temperatures are listed in **Table 1**.

Role of ferrite on cracking : Ferrite acts as a scavenger of the impurities during solidification and prevents fissuring in the weld metal. Matsuda et al. [16] summarised the probable reasons.

1. Ferrite has a greater solubility than austenite for harmful elements such as sulphur and phosphorous and thus the segregation of these elements at the grain boundaries is decreased.
2. Total grain boundary area is enlarged due to the presence of ferrite-austenite boundary together with austenite grain boundary.
3. Austenite grain size would be refined in a two-phase alloy containing ferrite.
4. Compositions forming some ferrite have a smaller solidification range than fully austenitic composition.
5. Contraction stress is reduced because of a smaller co-effcient of thermal expansion of ferrite.
6. Liquid films are dispersed by the existence of ferrite, and ferrite strengthens the grain boundary or prevents the formation or propagation of crack.
7. Ferrite suppresses polygonisation process.

Table – 2
Composition of Austenitic Stainless Steels

AISI No	%Cr	%Ni	%C Max.	Others
301	16-18	6-8	0.15	--
302	17-19	8-10	0.15	--
304	18-20	8-12	0.08	--
304L	18-20	8-12	0.03	--
305	17-19	10.5-13	0.12	--
309	22-24	12-15	0.20	--
310	24-26	19-22	0.25	1.5 Si max.
310S	24-26	19-22	0.08	1.5 Si max.
316	16-18	10-14	0.08	2-3 Mo
316L	16-18	10-14	0.03	2-3 Mo
321	17-19	9-12	0.08	(5 * %Ti) min.
347	17-19	9-13	0.08	(10 * %C)Nb+Ta min.

STAINLESS STEELS FOR CRYOGENIC APPLICATIONS

Austenitic stainless steels are commonly accepted structural materials for cryogenic applications. They have a wide range of mechanical properties, depending on their chemical compositions and thermo-mechanical processing. The popularity stems from their retention of excellent mechanical properties, particularly toughness at low temperatures coupled with ease of fabrication. Three general classes of these alloys are useful for cryogenic applications.

The AISI 300 series stainless steels : These grades have moderate strength, excellent toughness and good fabrication characteristics. Types 304 and 304L are the most commonly used alloys. Type 316 contains 2 to 3% Mo to improve resistance to pitting in chloride solutions, specially selected for piping systems for liquefied natural gas. AISI 316L is the low carbon grade desirable to avoid sensitization. Types 321 (alloyed with titanium) and 347 (alloyed with niobium and tantalum) are also sensitization-resistant grades.

Table – 3
Composition of Nitrogen added austenitic stainless steels

AISI No	%Cr	%Ni	%Mn	%C	%N
304N	18-20	8-10.5	2.0 max.	0.08	0.1-0.16
304LN	18-20	8-12	2.0 max.	0.03	0.1-0.16
316N	16-18	10-14	2.0 max.	0.08	0.1-0.16
316LN	16-18	10-14	2.0 max.	0.03	0.1-0.16

Table – 4
Comparison of chemistry of E 308L under different standards

Standard	Code	%C	%Cr	%Ni	%Mo	%Mn	%Si	%P	%S	%Cu
SFA 5.4	E308L	0.04	18-21	9-11	0.75	0.5-2.5	0.9	0.04	0.03	0.75
BS 2926	E19.9L	0.04	18-21	9-11	0.5	0.5-2.5	1.0	0.04	0.03	--
DIN 8556	E19.9nC	0.04	18-21	8-11	--	2.0	1.5	0.03	0.025	--
ISO3581	E19.9L	0.04	18-21	8-11	--	--	--	--	--	--
IS5206	E19.9L	0.04	18-21	8-11	0.5	2.5	0.9	0.04	0.03	--

Note : **1.** Single values shown are maximum percentages. **2.** Dashed line indicates value not mentioned.

Table – 5
Comparison of chemistry of E 316L under different standards

Standard	Code	%C	%Cr	%Ni	%Mo	%Mn	%Si	%P	%S	%Cu
SFA 5.4	E316L	0.04	17-20	11-14	2-3.0	0.5-2.5	0.9	0.04	0.03	0.75
BS2926	E19.12.2L	0.04	17-20	11-14	2-2.5	0.5-2.5	1.0	0.04	0.03	--
DIN8556	E19.12.3nC	0.04	17-20	10-13	2.5-3	2.0	1.5	0.03	0.025	--
ISO3581	E19.12.2L	0.04	17-20	11-14	2-2.5	--	--	--	--	--
IS5206	E19.12.2L	0.04	17-20	11-14	2-2.5	2.5	0.9	0.04	0.03	--

Note : **1.** Single values shown are maximum percentages. **2.** Dashed line indicates value not mentioned.

Table – 6
Comparison of mechanical properties of E308L and E316L under different standards

Standard	UTS(MPa)	EL(%)	CVN(J)	LE(mil)	UTS(MPa)	EL(%)	CVN(J)	LE(mil)
SFA 5.4	520	35	--	15	490	30	--	15
BS2926	510	30	--	--	500	25	--	--
DIN8556	--	--	40	--	--	--	40	--
ISO3581	--	--	--	--	--	--	--	--
IS5206	510	30	--	--	490	--	--	--

Type 310S is a low carbon version of AISI type 310 and useful where dimensional stability and non-magnetic behaviour is essential. The chemical compositions of these grades are shown in **Table 2**.

The nitrogen strengthened steels : Nitrogen increases the yield strength of austenitic stainless steels, particularly for cryogenic temperatures. Low temperature strength and ductility are higher than those for stainless steel without nitrogen. The deliberate addition of nitrogen is in the range of 0.10 to 0.16% for 304N and 316N according to the United States specification. The corresponding European specification permits nitrogen levels upto 0.25%. Sometimes manganese is used in these grades to replace part of the nickel content and also to increase the solubility of nitrogen in austenite. The chemical compositions are shown in **Table-3**.

Cold rolled sheets of AISI 300 series grades : These are high strength sheet materials, formed by the cold-working operations of AISI grades 301, 302, 304L and 310. The materials are for specialised applications like missile cases operating at $-253^{o}C$ (liquid hydrogen) or $-187^{o}C$ (liquid oxygen).

The first two grades are readily weldable by all common welding techniques utilising appropriate consumables and procedures, but weldability of the cold rolled grades is poor in comparison to the other two.

COMPARISON OF DIFFERENT STANDARDS

AWS E 308L and E 316L are the widely used grades of electrodes for satisfactory cryogenic applications. The comparison of the all-weld chemistry of these two grades with Indian and other overseas standards is shown in **Table 4 & 5**.

The mechanical property requirements of the weld metal as per different specifications are shown in **Table 6**. Only in DIN 8556, the absorbed energy is mentioned at $20^{o}C$ and in SFA 5.4 the lateral expansion at $-196^{o}C$.

DESIGN CHARACTERISTICS OF WELDING CONSUMABLES FOR CRYOGENIC SERVICE

Solidification Modes

The different modes of weld metal solidification depend on composition, as indicated in **Fig. 3**. The growth of the dendrites and morphology of the ferrite formed are also discussed in Section 2.1 and shown in **Figs. 3 & 4**. The primary solidification phase is sensitive to both composition of the weld and the thermal conditions of the solidification. Austenite (A) and austenite-ferrite (A-F) modes occur at $Cr_{eq}/Ni_{eq}<1.5$. In fully austenitic mode, ferrite does not form. Austenite is the primary phase in A-F solidification and partial transformation to eutectic ferrite takes place from the remaining liquid. F-A and F modes result from Cr_{eq}/Ni_{eq} ratio above 1.5. With progressive increase in the ratio, the structure changes to vermicular, lacy, acicular, and Widsmantatten types.

The elements influence solidificaion cracking through the solidification modes. The segregants at the grain boundaries influence the grain wettability conditions and are considered to be one of the main reasons for the difference in cracking susceptibility between solidification modes.

Controlled Ferrite

The presence of ferrite in ASS weld metal imparts an important role to determine the weldability and service performance of a welded structure. Ferrite, if present in weld metals, can reduce sensitivity to hot cracking and fissuring [1,17,18,19]. A higher ferrite content in weld metal decreases ductility and impact strength at cryogenic temperatures and therefore, is undesirable for cryogenic applications [16,19,20 to 25]. Higher ferrite also decreases corrosion resistance of the weld metal.

The minimum ferrite limit necessary to ensure freedom from cracking depends, among other factors, on the weld metal

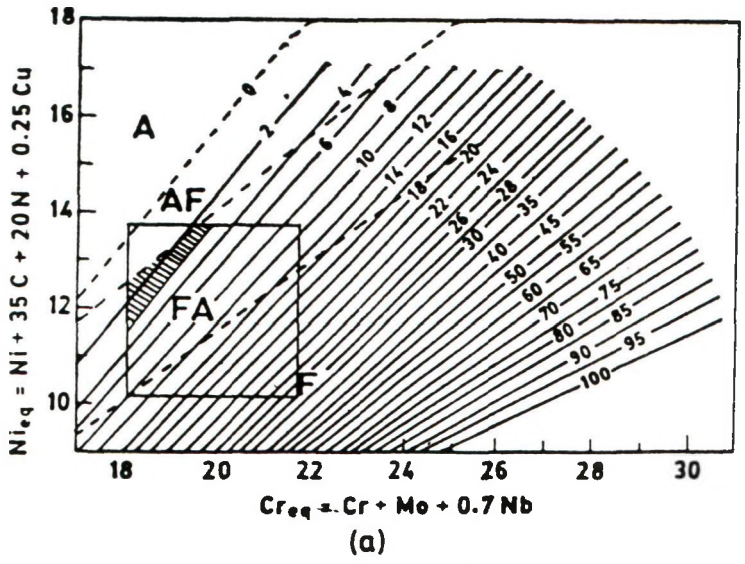

Fig. 9 : The composition window of (a) E-308-L superimposed on WRC-1992 constitution diagram. The shaded area shows the composition zone meeting the cryogenic specifications.

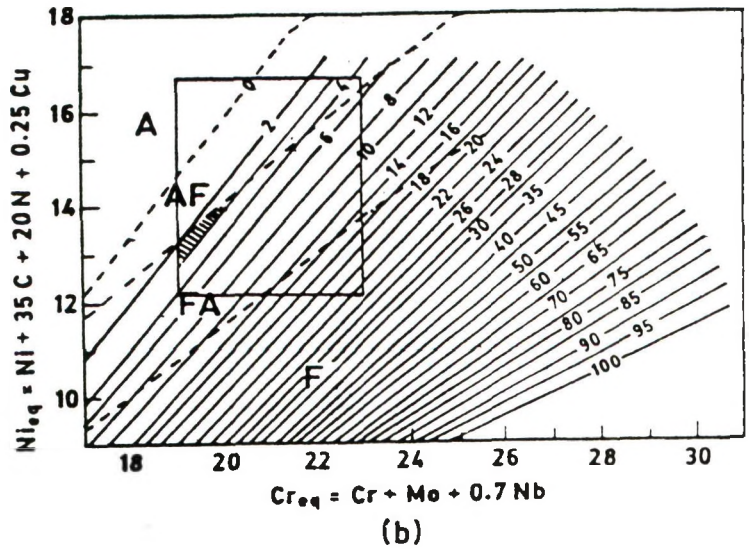

Fig. 9 : The composition window of (b) E-316-L superimposed on WRC-1992 constitution diagram. The shaded area shows the composition zone meeting the cryogenic specifications.

composition. The amount of ferrite required to be present for cryogenic applications is a function of quantity of oxygen in the weld metal. High ferrite can be tolerated to meet the minimum lateral expansion (15 mils) if the weld metal contains low oxygen. The lower and upper limits of nickel equivalents and chromium equivalents of weld metals of E 308L and E 316L are plotted in WRC 1992 diagram as shown in **Figs. 9a** & **9b** respectively. The shaded area in each figure represents the range of weld metal compositions solidifying in ferrite-austenite modes with the maximum specified ferrite (3 FN) to meet various specifications for cryogenic applications. Nitrogen reduces or eliminates ferrite in ASS weld metals designed to have certain amount of ferrite in the microstructure. This phenomenon is observed during different positional welding, where the variation in arc gap changes the level of nitrogen pick-up that imparts a pronounced effect on delta ferrite (**Fig. 10**).

Mechanical Properties

Welding produces marked changes in the microstructure of austenitic stainless steels. Heat affected zone adjacent to the welds suffers from precipitation of chromium carbides to varying degrees. This precipitation of carbides, known as sensitization, depends on the carbon content and the exposure time in the range of 420 to 870°C (26).

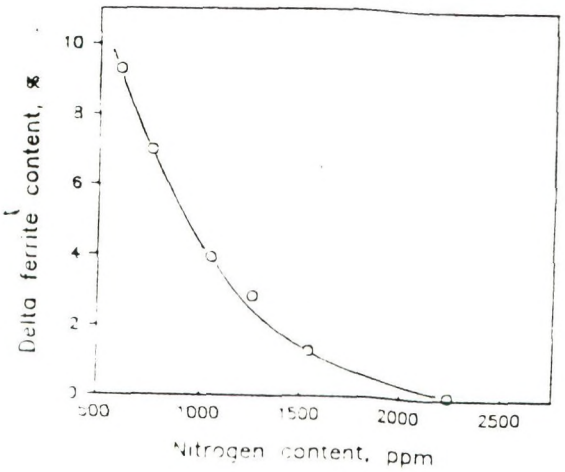

Fig. 10 : Change in the delta ferrite content of the weld metal with nitrogen content [19]

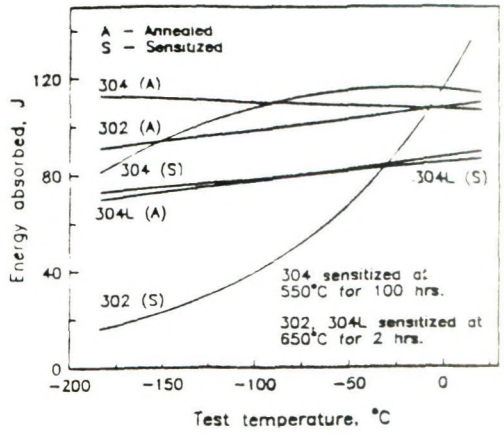

Fig. 11 : Results of Charpy keyhole impact test on annealed and sensitized conditions [26]

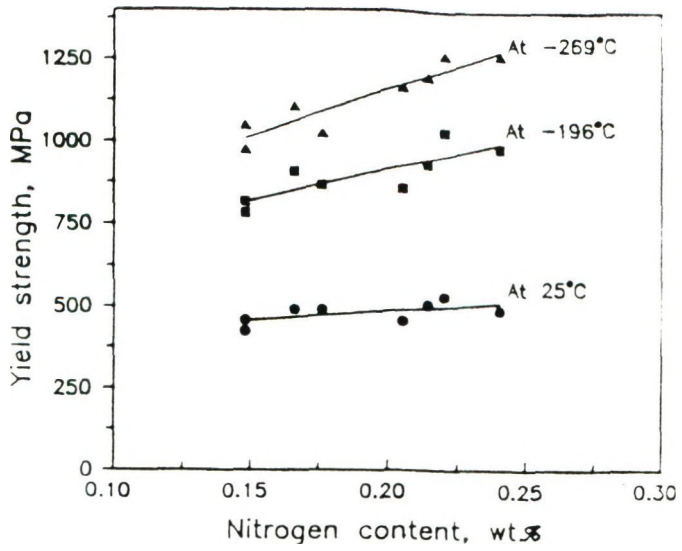

Fig. 12 : Yield strength versus nitrogen for type 316LN welds at 25°C, –196°C and –269°C [27]

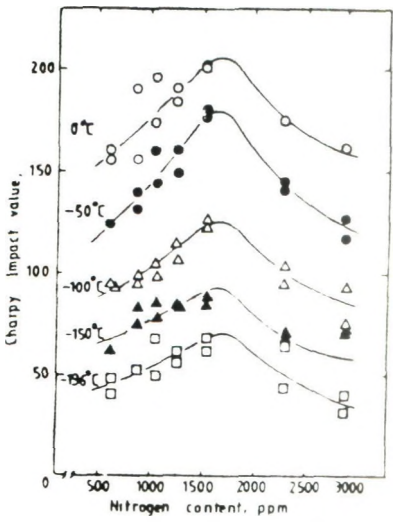

Fig. 13 : Effect of nitrogen content on the charpy impact value of the weld metal at different test temperatures [19]

Sufficiently available carbon in welds tends to enhance the situation and is detrimental to toughness of the steel (21). Impact test data of Type 302, 304 and 304L steels (**Fig. 11**) describe the effect for annealed and sensitized conditions. The figure shows that in relatively high carbon (0.15% max.) type 302 steel, the sensitization treatment markedly reduces toughness at –196°C. However, the toughness of lower carbon types 304 and 304L steels remains relatively

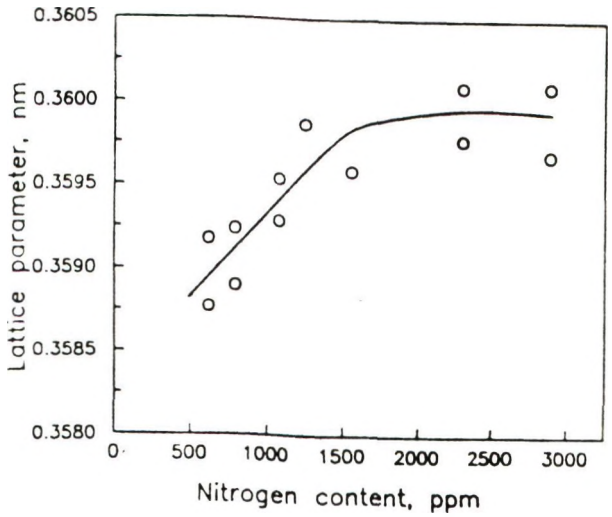

Fig. 14 : Change in the lattice parameter of the austenite matrix of weld metal with nitrogen content [19]

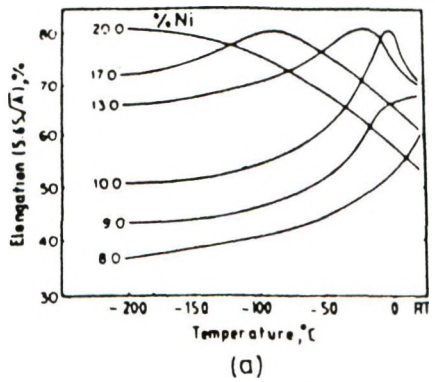

(a)

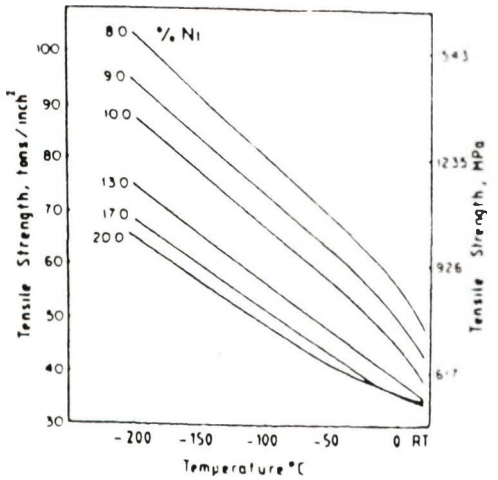

(b)

Fig. 15 : Effect of nickel on mechanical properties of ASS at subzero temperatures; (a) on ductility and (b) on tensile strength [26]

high after sensitization. In multipass weldments, the underlying weld beads may receive sufficiently long exposures in the sensitization temperature range. So, to avoid the precipitation of carbides, weld metals containing very low carbon are commonly used for cryogenic applications.

The presence of nitrogen in weld metal stabilises the austenite and gives rise to interstitial solution hardening (27). This results in increase in the yield strength of austenitic weld metals at or below room temperature (**Fig. 12**). Withrell et al. (28) studied the effect of nitrogen on weld metal in 304LN plate welded with 316L electrode. The precipitation of nitride, carbo-nitrides at the grain boundaries are reported and are believed to contribute to low temperature brittleness. A similar observation was obtained by McCowan et al (29) with 308L weld metal at liquid nitrogen temperature. Nitrogen content beyond 0.16wt% in 308L SMA welds at cryogenic temperatures caused a substantial decrease in absorbed energy and at 0.25 wt% N, the absorbed energy was reduced to approximately 50%. Although it is reported that nitrogen decreases toughness at cryogenic temperatures, there are contradictory opinions too. Enjo et al. (19) claim judicious addition of nitrogen is beneficial for low temperature impact properties of 304 type austenitic stainless steel weld metals deposited by lime-

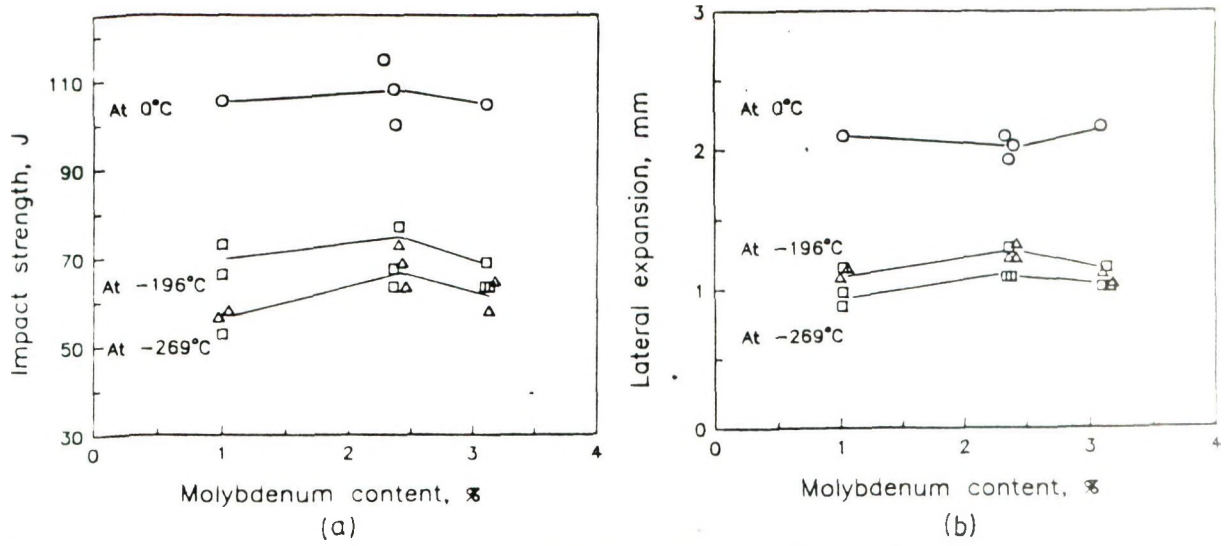

Fig. 16 : Effect of molybdenum content on (a) absorbed energy and (b) lateral expansion of weld deposits with 0.06%C [31]

titania type covered electrodes. They carried out Charpy tests at different temperatures with varying N_2 content. The impact value of weld-metal was found to increase with increasing N_2 content upto 1700-1800 ppm, beyond which the impact value fell (**Fig. 13**) due to percipitation of nitrides.

The lattice parameters are enlarged by nitrogen upto 1600 to 1700 ppm, as shown in **Fig. 14**. The graph shows the maximum pick–up of nitrogen in austenite and justifies the increase in toughness upto 1600 to 1700 ppm.

Nickel has a strong influence on mechanical properties between room temperature and cryogenic temperature (**Fig. 15**). Higher nickel increases ductility (**Fig. 15a**) and permits more strain hardening to occur before fracture. The tensile strength is increased with decrease in nickel content due to instability or transformation of austenite to martensite (26) as can be seen from **Fig. 15b**. Nickel raises toughness by 3 J for each percent, while chromium has a negative effect of about 1.2 J for each percent. Siewert (30) statistically correlated the effect of alloying elements on toughness at −196°C.

$$Cvn(J) = 19 - 1.4FNCS - 890C^2 + 1.4Ni$$

where, FNCS is the ferrite no. calculated according to the Schaeffler Diagram.

Manganese slightly increases the yield strength at liquid helium temperature as reported by McCowan et al, (29). A combined effect of Mn and N_2 in the range of 1.5 to 10 wt% and 0.04 to 0.26 wt % respectively is expressed as :

$$\text{Weld YS(MPa)} = 360 + 3400(wt\%N) + 14(wt\%Mn)$$

It has a minor effect on cryogenic toughness, but lateral expansion is decreased with increase in Mn content.

Molybdenum is a ferrite former and tends to restrict austenite formation. An increase in YS, improved effect on CVN absorbed energy and lateral expansion with Mo addition is reported by Matsumoto et al. (31) on 17.5Cr, 16.5Ni, 6.5Mn, 2.3Mo steel. The results are shown in **Figs. 16a** & **16b**. But in ASS for cryogenic applications its addition is restricted to 2-3% range as it gives rise to segregation and appears to be detrimental to impact lateral expansion.

Niobium and Titanium are the most potent carbide formers and have deleterious effect on cryogenic toughness.

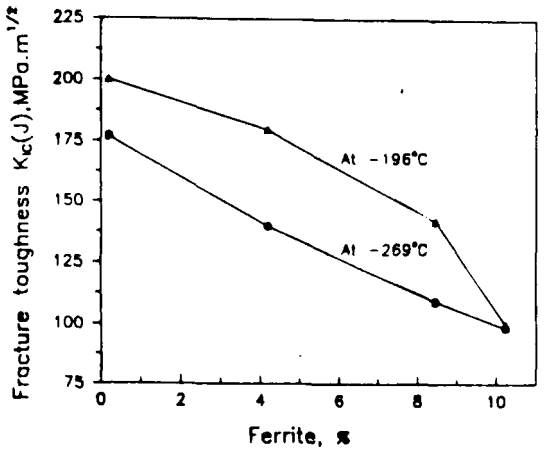

Fig. 17 : Fracture toughness of AWS 316 and 316L weld metals at −196° and −169°C as a function of ferrite content [20] and the oxygen content in the weld metal [33]

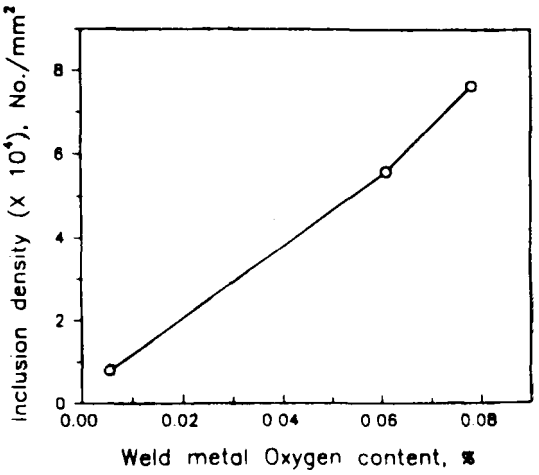

Fig. 18 : Relationship between the inclusion density and the oxygen content in the weld metal [33]

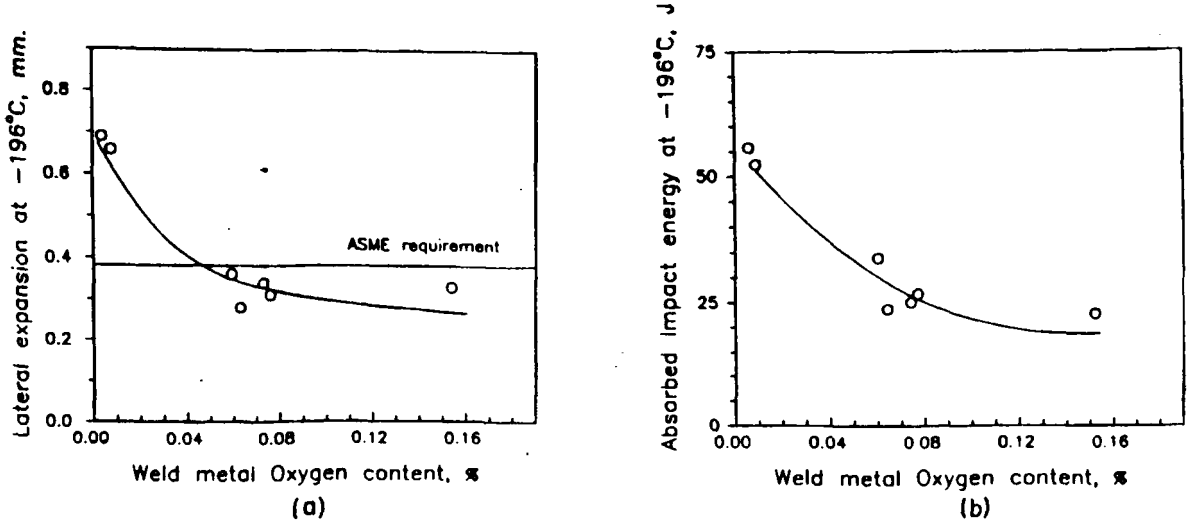

Fig. 19 : The effect of oxygen content on the impact properties of ASS weld metal at −196°C, (a) lateral expansion and (b) impact energy [33]

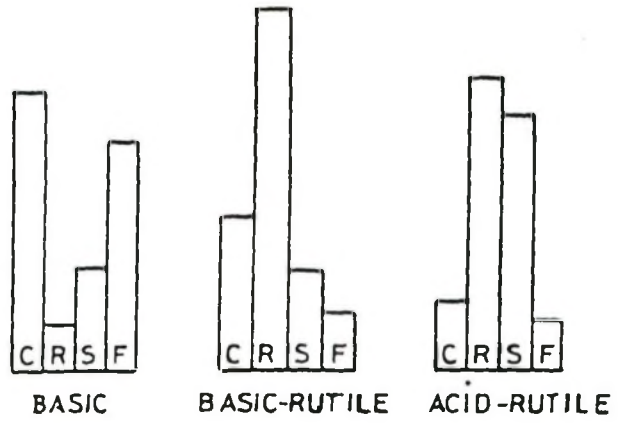

Fig. 20 : Relative proportion of major constituents of different electrode coatings [22]

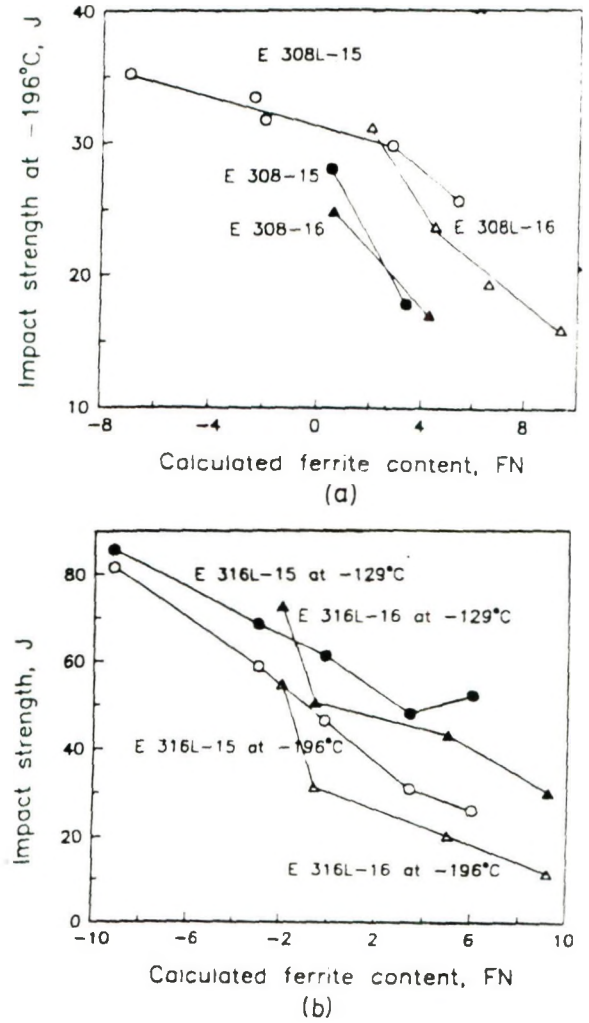

Fig. 21 : Impact strength versus ferrite number for (a) 308/308L and (b) 316/316L grade electrodes at -196°C [35]

Szumachowski and Reid (20) have shown that ferrite reduces toughness at -196°C for a wide range of stainless steel weld metals. A decreasing trend of fracture toughness for 316L weld metal at -269°C and -196°C with increase in ferrite percentages (**Fig. 17**) is reported.

Inclusions

The toughness of austenitic stainless steel weld metal at cryogenic temperatures is significantly lower than that of the corresponding base metal. Some of the metallurgical factors that cause this low toughness in weld metal are well-known, such as precipitates of carbides and nitrides, intermetallic compounds, the presence of delta-ferrite and inclusions.

The presence of phosphorus and sulphur in weld metal forms inclusions and enhances the crack susceptibility. In the AISI 300 series alloys it is well recognised

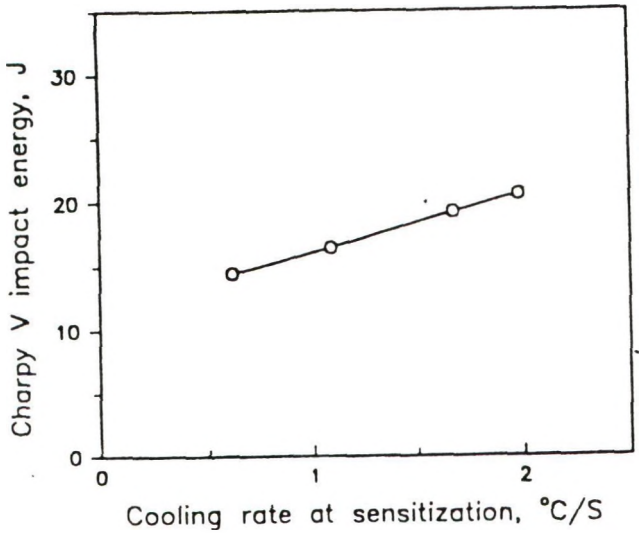

Fig. 22 : Charpy V notch impact energy at −196°C as a function of cooling rate for 316L weldments at 8 ± 2% ferrite [21]

that both P and S are largely responsible for the formation of low melting eutectic films which form weld hot cracks (32). The most important factor in determining the effect of impurities is not necessarily the quantity of impurity present, but rather the nature of the phases formed by the impurity.

Welds have a high inclusion content due to contamination from the slag. Siewert and McCowan (27) evaluated the data from two gas metal arc weld (316L and 18Cr-20Ni) compositions at different levels of inclusion content by varying the oxygen potential of shielding gas. An inverse correlation between the toughness and the inclusion spacing (inverse root of inclusion area density) was established.

The effect of oxygen is very pronounced in causing an increase in inclusions in the weld metal. Kim et al. (33) quantified the amount of inclusion in terms of inclusion density and plotted as a function of O_2 content (**Fig. 18**). The figure shows almost a linear relation between oxygen content and inclusion density in the range studied. The O_2 content in welds also reduces both Charpy and lateral expansion values at -196°C, as shown in **Figs. 19a** & **19b**.

There is a combinational condition of oxygen and ferrite contents to meet the minimum lateral expansion (15 mils) and less ferrite is required for high oxygen weld metal to meet ASME specification i.e., low oxygen weld metal can meet the above

Table – 7
Melting points of some RE compounds

Compound	Melting point(°C)
Ce_2S_3	2150
La_2S_3	2100
CeS	2100
LaS	1970
Ce_2O_2S	1950
La_2O_2S	1940

standard, even with high ferrite content.

Type of Coating

Both rutile and basic coatings are commonly used for austenitic stainless steel electrodes. Marshall et al. (22) have shown the relative proportions of major flux minerals in the electrode coatings suitable for cryogenic applications (**Fig. 20**).

Although rutile coated electrodes have smooth arc, good slag detachability, and pleasing operating characteristics in a wider range of welding currents, lime coated electrodes contain fewer non-metallic inclusions in the weld metal than the former.

Nitrogen pick-up during welding due to improper shielding is undesirable, especially in welds for cryogenic applications. This causes to change the level of residual delta-ferrite (**Fig. 10**) that may be required to get a crack-free weld deposit (34). Even with good welding techniques, nitrogen pick-up is 35% to 75%

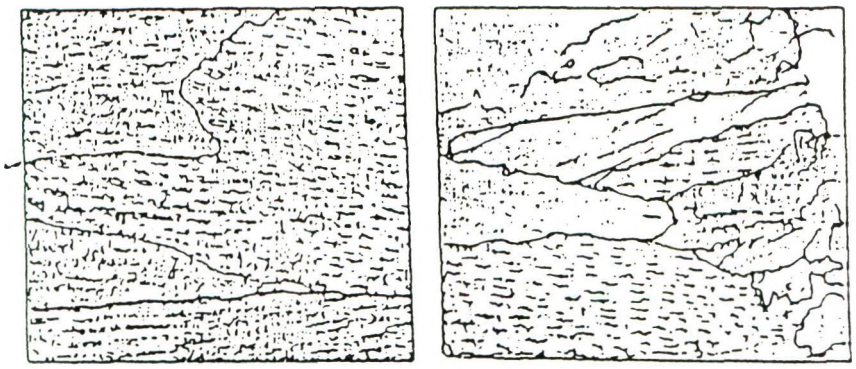

Fig. 23 : The microstructure of 15Cr25Ni6Mo austenitic weld metal (a) non-modified and (b) modified with REM [42]

more in titania covered electrodes (35).

The mineral rutile contains 0.2 to 0.7% each of niobium and vanadium oxides. Transfer of these two elements increases with deoxidant addition and accounts for the reverse effect on the toughness of the weld deposits. **Figs. 21a** & **21b** relate the toughness and FN with type of coating for 308L and 316L electrodes.

Heat Input

Higher heat input in the welding processes imparts a deleterious effect on the weld metal as well as on base metal. Austenitic stainless steels have poor thermal conductivity and high coefficient of thermal expansions, therefore, special care is needed for successful welding.

Sensitization takes place in the bottom layers of multi-pass welding if the interpass temperature is not carefully controlled. The grain boundaries may become associated with carbides and carbonitrides during reheating the previously deposited beads by subsequent passes. These precipitates are responsible for intergranular brittleness and also enhance the micro-fissuring propensity of the welds leading to premature failure (28).

Dilution with base metal and the rate at which the weldments cool through the two-phase austenite plus ferrite region can have a significant effect on both the ferrite distribution and morphology (24,36). The morphology of ferrite also changes from isolated patches at low heat-input welds to a continuous ferrite phase at higher heat-input welds (21). Decreased cooling rate increases the ferrite dendritic spacing and the effective grain size of the austenitic matrix, and decreases the Charpy impact toughness at - 196°C (**Fig. 22**). In multipass welds of thick sections, repeated thermal cycles may transform previously formed delta ferrite to sigma phase (37) that significantly decreases the impact toughness at -196°C.

ADDITION OF RARE EARTH METALS

Rare earth metals (REM) in welding consumables (wires and fluxes) are highly promising. They are excellent deoxidisers and de-sulphurisers. According to Abralov et al. (38), 67-75% lower concentration of sulphur and 33-41% reduction in oxygen is obtained in deposited weld metal with REM, compared to where no REM addition is made.

During solidification after welding, REMs preferentially concentrate at the grain boundaries on cooling that retard the diffusion of some elements (C, Si, Mo) towards the grain boundary. This lowers the segregation of brittle phases ($Mo_5Cr_6Fe_{18}$), and silicate inclusions (39). Rare earth concentrates at the liquid-solid interface during solidification, and decreases the length of columnar zone. RE inclusions also act as nuclei, thereby refining the grain structure (40-42). The effect of REM on the grain refinement is shown in **Figs. 23a** & **23b**.

The presence of REM in electrode coating also improves the cracking resistance of austenitic stainless steel weld metals (39-43). The plasticity of the weld metal with RE is higher than that without RE. Zhao Neghuai et al. (39) have reported an increase of even 50% in the Charpy value of the weld metal with REM addition, tested at –196°C.

An optimum amount of rare earth spherodises the thin elongated MnS inclusions (m.p.=1600°C), which reduces the degree of stress concentration and lowers the susceptibility to sulfide stress corrosion cracking.

Segregation of low melting impurities at the grain boundaries often results in solidification cracking. Though solubility of impurity elements in ferrite is more than in austenite, the amount of these elements is restricted for cryogenic applications. REs have strong affinity for sulphur compared to manganese, so the MnS inclusions are replaced by RE sulphides and oxysulphides which are of higher melting point and also thermodynamically more stable. This improves the hot cracking resistance also. The melting points of some common RE compounds are given in **Table 7**. But addition of RE beyond a certain optimum amount exerts some negative effect also. The grain size increases, accumulation of coarse particles of complex oxysulphides of REs are formed in the fusion zone, and the capacity of welds for resisting formation of tears decreases.

SUGGESTED GUIDELINES

a) Fully austenitic weld metal with very low carbon is usually preferred to avoid sensitization, as it deteriorates the cryogenic toughness.

b) Nitrogen is controlled to 0.15% maximum in welds to achieve necessary strength level as well as to restrict its deleterious effects.

c) Sulphur, phosphorus and oxygen should be as low as possible to reduce the volume fraction of inclusions and also to reduce solidification cracking.

d) Manganese interacts with sulphur and nitrogen but beyond a certain limit reduces lateral expansion, so should be controlled within 1.5 to 2.5%.

e) Nickel and Chromium should be balanced with other alloying additions to get a ferrite level of 2 to 3 FN conforming to the specifications.

f) Niobium and titanium additions are avoided because of their detrimental effect on toughness.

g) Molybdenum should be kept in the range of 2-3% for E-316L, above which segregation effect predominates.

h) Based on the amount of inclusion, optimum rare earth can be added to improve the properties of weld metal.

i) Lime type electrodes are preferred over rutile type.

j) Smaller diameter electrodes should be used for better arc protection and low heat input.

SUMMARY

Low carbon austenitic stainless steels are commonly used for cryogenic applications. The electrodes used to successfully weld these steels should match the mechanical properties of the base plate and should also be free from solidification cracking.

The chemical composition of the all-weld deposit is to be carefully selected to obtain $Cr_{eq}/Ni_{eq}>1.5$

for primary ferritic solidification mode. The amount of ferrite in weld metal is controlled between 2-3 FN. Nil ferrite may cause micro-fissuring but on the other hand, high ferrite will reduce cryogenic toughness.

A continuous ferrite network may result from high heat input welding. This type of structure is undesirable, as it provides an easy path to failure. Therefore, lower diameter electrodes are preferred to obtain low heat input. Moreover, high heat input may also cause sensitization in the previously deposited passes in multi-layer deposits.

Although the inclusions are detrimental to cryogenic toughness, the nature of the phases formed is more important. A basic type flux composition is usually preferred due to lower level of oxygen in the weld metal. Basic type coatings also cause less nitrogen pick-up than titania covered electrodes during welding.

A profound influence of rare earth metals on properties of weld metal is found. They can be added in the welds through the flux coverings. REMs preferentially react with sulphur and oxygen and change the formation, shape and the distribution of non-metallic inclusions. An optimum addition of 0.2 to 0.4% RE-oxides in flux coverings is highly beneficial in increasing mechanical properties and cryogenic toughness.

ACKNOWLEDGEMENT

The authors acknowledge the help of Department of Science and Technology, Government of India for financial assistance to this work done under investigation on Indigenisation of Special purpose Welding consumables.

REFERENCES

1. Kotecki, D.J. and Siewert, T.A., WRC – 1992 Constitution Diagram for Stainless Steel Weldmetals: A modification of the WRC-1988 Diagram. Welding Journal, 1992(5): 171S-178S.
2. Guina, R.B. and Ratz, G.A., The measurements of delta ferrite in ASS, WRC bulletin 132 August 1968.
3. DeLong, W.T., Discussion of the International testing program for the determination of ferrite content in ASS weld metal, Doc.II C 331-70.
4. Japanese delegation, On the measurements of ferrite content in deposited metals of ASS Doc. II C 311-70.
5. Dutch delegation, Possible methods for determining the ferrite content of stainless steels. Doc. II C 167 64.
6. Schwartzendruber, L.J., Bennett, L.H., Schoefer, E.A., DeLong, W.T. and Campbell, H.C., Mossbauer-effect examination of ferrite in stainless steel welds and castings, Welding Journal, 1974(1).
7. DeLong, W.T., Ferrite in ASS weld metal, 1974 Adams lecture publication, No. 1227 of the AWS Doc.II C 481-76.
8. Stalmasek, E., Calibration of instruments for magnetic measurements of the delta ferrite content in austenitic CrNi weld metals, Doc. II C 257-67.
9. Entin, S.D., The magnetic method of quantitative determination of delta ferrite in weld metal - Present state and development in the USSR. Doc. II C 401-73.
10. DeLong, W.T., Ostrom, G.A. and Szumachowski, E.R., Measurement and calculation of ferrite in S.S.weld metal, Welding Journal, 1956(11).
11. Arata,Y., Matsuda, F, Katayama, S., Nakagawa, H, Ogata, S., Solidification crack susceptibility in weld metals of fully ASS Trans, Japan Welding Res. Inst. 1:5, Nr 2 33-51(1976); Report II 6 Nr.1 105-116(1977); Report III.6 Nr 2 37-46 (1977); Report IV : 7 Nr.2 21-24 (1978); Report V:10 Nr.2 73-84(1981); Report VI :11 Nr 1 79-94 (1982).
12. Apblett, W.R., Pellini, W.S., Factors which influence weld hot cracking, Welding Journal, 33 (83-90)S, 1954.
13. Hull, C.F., Effects of alloying additions on hot cracking of ASS Proc. American Soc. Test.Mat.60. 667-690 (1960).
14. Borland, J.C., Younger, R.N., Some aspects of cracking in Cr-Ni austenitic steels, British Weld Journal, 7,22-59, (1960).
15. Thomas, R.D., HAZ cracking in thick sections of austenitic steels-part 1, Welding Journal, 63, 12, 24-32. (1984); part 2, Welding Journal 63, 355S-368S, 1984.
16. Matsuda, F., Nakaguda, H., Vehara, T., Katayama, S. and Arata, Y., A New Explanation of Role of Delta-ferrite Improving Weld Solidification Crack Susceptibility in ASS. Transactions of JWRI, Vol. 8, No.1, 1979: 17-24.
17. Brooks, J.A., Effect of P,S and ferrite content on weld cracking of type 309 SS., Welding Journal. 1978(5), (139-143)S
18. Siewert, T.A., McCowan, C.N. and Olson, D.L., Ferrite Number Prediction to 100 FN in

Stainless Steel Weldmetal. Welding Journal, 1988(12):289S-298S.

19. Enjo, T., Kikuchi, Y. and Moroi, H., Influence on Structure and Low Temperature impact Properties of 304 Type Austenitic Stainless • Steel Weldmetals by SMAW Process. Welding Research Abroad, 1981(6-7): 34-41.
20. Szumachowski, E.R. and Reid, H.F., Cryogenic Toughness of SMA Austenitic Stainless Steel Weldmetals: Part 1-Role of Ferrite, Welding Journal, 1978(11): 325S-333S.
21. Read, D.T., McHenry, H.I., Steinmeyer, P.A. and Thompson, Jr., R.D., Metallurgical Factors Affecting the Toughness of 316L SMA Weldments at Cryogenic Temperature, Welding Journal, 1980(4): 104S-113S.
22. Marshall, A.M., Farrar, J.C.M., Effects of Residual Impurity and Micro-alloying Elements on Properties of Austenitic Stainless Steel Weldmetals. Metal Construction, 1984(6):347-353.
23. Menon, R. and Kotecki, D.J., Literature Review - Nitrogen in Stainless Steel Weldmetal. WRC Bulletin 369.
24. DeLong, W.T., Ferrite in Austenitic Stainless Steel Weldmetal. Welding Journal, 1974(7): 273S-286S.
25. Reid, H.F. and DeLong, W.T., Making Sense out of Ferrite Requirements in Welding Stainless Steels, Metal Progress, 1973(6): 284-286.
26. Brickner, K.G. and Defilipi, J.D., Mechanical Properties of Stainless Steels at Cryogenic Temperatures and at Room Temperature, Handbook of Stainless Steels, McGraw Hill Book Company, 1977:20.1-20.38.
27. Siewert, T.A. and McCowan, C.N., Joining of ASSs for Cryogenic Applications, Advances in Cryogenic Engineering Materials, Volume-38, Plenum Press, New York, 1992, 109-115.
28. Withrell, C.E., Welding Stainless Steels for structures Operating at Liquid Helium Temperature. Welding Journal, 1980(11): 326S-342S.
29. McCowan, C.N., Siewert, T.A., Reed, R.P. and Lake, F.B., Manganese and Nitrogen in Stainless Steel SMA Welds for Cryogenic Service. Welding Journal, 1987(3):84S-92S.
30. Siewert, T.A., Predicting the Toughness of SMA Austenitic Stainless Steel Welds at -196°C. Welding Journal, 1986(3):23-28.
31. Matsumoto, T., Satoh, H., Wadayama, Y. and Hataya, F., Mechanical properties of Fully Austenitic Weld Deposits for Cryogenic Structures. Welding Journal, 1987(4):120S-126S.
32. Brooks, J.A., Thompson, A.W. and Williams, J.C., Weld Cracking of Austenitic Stainless Steels - Effects of impurities and Minor Elements. Physical Metallurgy of Metal Joining. The Metallurgical Society of AIME Publications, 1980:117-136.
33. Kim, J.H.,Oh, B.W., Young, J.G., Bahng, G.W. and Lee, H.M., Effects of Oxygen Content on Cryogenic Toughness of ASS Weldmetal. Advances in Cryogenic Engineering, Volume-36, Plenum Press, New York, 1990:1339-1346.
34. Long, C.J. and DeLong, W.T., The Ferrite Content of ASS Weldmetal. Welding Journal, 1973(7): 281S-297S.
35. Szumachowski, E.R. and Reid, H.F., Cryogenic toughness of SMA ASS Weldmetals: Part II-Role of Nitrogen. Welding Journal, 1979(2):34S-44S.
36. Lippold, J.C. and Savage, W.F., Solidification of ASS Weldments: Part 2- The effect of Alloy Composition on Ferrite morphology. Welding Journal, 1980(2): 48S-58S.
37. Yushenko, K.A., Savchenko, V.S., Solokha, A.M. and Voromin, S.A., Effect of Delta-Ferrite on Properties of Welds in Austenitic Steels at Cryogenic Temperatures. Advances in Cryogenic Engineering, Volume-40, Plenum Press, New York, 1994:1263-1266.
38. Abralov, M.A., Sergeev, V.G. and Borisova, N.N., The Effect of Cerium and Yttrium on the Structure and Properties of Weldmetal in 06KhN28MDT A. Automatic Welding, 1978, Volume-31, No. 9.
39. Nenghuai, Z., Dianming, L., Jingkai, J. and Lianfang, X., Effect of Rare Earths on Crack Resistance of ASS Weldmetal. New Frontiers in Rare Earth Science and Application. Science Press, Beijing, China, Academic Press, INC, Volume-II, 1985: 1294-1296.
40. Ruizhen, G., Hanqi, H and Xueyou, Z., Effects of Rare Earth Elements on Solidification of Steels. New Frontiers in Rare Earth Science and Application. Science Press, Beijing, China, Academic Press, INC, Volume-II, 1985:1277-1282.
41. Musiyachenko, V.M et al., Effect of non-metallic inclusions with rare earth metals on the structure and properties of weld metal in welding high strength steels, Welding International, 1988 No. 4.
42. Geller, A.B. and Kakovkin, O.S., Metallurgical features of reduction of rare earth metals from their oxides in welding with coated electrodes. Welding Production, 1986, Volume-33, No.10.
43. Kiryakov, V.M. et al., The effect of micro-alloying austenitic welds with cerium on their resistance to the formation of cold cracks in the fusion zone. Automatic Welding, 1979 Volume 32 No. 10.